LA-UR-87-3092
(Final)

Los Alamos National Laboratory is operated by the University of California for the United States Department of Energy under contract W-7405-ENG-36

LA-UR--87-3092

DE88 003185

TITLE PRELIMINARY INJECTOR, ACCELERATOR, AND BEAMLINE DESIGN FOR RF-LINAC-DRIVEN XUV FREE-ELECTRON LASERS

AUTHOR(S): Bruce E. Carlsten and K. C. Dominic Chan

SUBMITTED TO Ninth International Free-Electron Laser Conference
Williamsburg, VA
September 14-18, 1987

DISCLAIMER

Los Alamos Los Alamos National Laboratory
Los Alamos New Mexico 87545

PRELIMINARY INJECTOR, ACCELERATOR, AND BEAMLINE DESIGN FOR RF-LINAC-DRIVEN XUV FREE-ELECTRON LASERS*

Bruce E. CARLSTEN and K. C. Dominic CHAN, MS-H825

Los Alamos National Laboratory, Los Alamos, NM 87545

The proposed Los Alamos National Laboratory XUV free-electron laser (FEL) facility requires exceptional beam quality at high peak currents.

Although the beam quality needed for a demonstration machine lasing at 50 nm is not far from what can be expected with extensions of present linacs to higher energy, conventional injector technology will not meet the requirements needed for lasing at 12 or 4 nm.

We have conceived a preliminary injector and accelerator design that will meet these requirements. Using the Los Alamos photoelectric injector, it appears that normalized 90% emittances of 24 π·mm·mrad can be attained in a relatively straightforward manner, and emittances down to 4 π·mm·mrad are possible. Beamline simulations have been performed with the particle-pushing code PARMELA, using particle-dump inputs from the particle-in-cell code ISIS. The latter models the photoelectric gun up to the range between 0.75 and 1 MeV.

Designs including electron guns with Pierce geometries have also been studied. Using an injector with a large planar-cathode Pierce gun seems to satisfy the 50-nm lasing requirements. We believe it could serve as a reliable backup to the photoelectric injector for the demonstration machine.

In addition, other beamline questions have been studied. Beamline bends have been designed that are achromatic and nearly isochronous. The threshold for cumulative beam breakup and the emittance growth caused by transverse resistive-wall beam instability have been calculated.

Finally, we discuss the advantages and disadvantages of building a straight-line machine versus a recycling machine, including recycling instability current levels.

*Work supported by the Division of Advanced Energy Projects, U.S. Dept. of Energy, Office of Basic Energy Sciences.

1. Introduction

The Los Alamos National Laboratory is proposing to construct an XUV FEL system extending from 1 nm to 400 nm, as a users facility [1]. In this paper we will discuss some of our ongoing accelerator calculations to evaluate preliminary design options. Computer simulations were done with the particle-pushing code PARMELA and the particle-in-cell code ISIS.

Section 2 will review the electron beam requirements determined from theoretical FEL interaction studies. In sections 3, 4, and 5 we will present two potential accelerator designs meeting these requirements by varying degrees. The first design uses the Los Alamos photoelectric injector and the second, primarily intended as a backup, uses a conventional Pierce gun. Both designs employ magnetic phase compression to bunch the beam to the final peak current and apertures for emittance filtering.

In section 6, calculations concerning various beamline mechanisms for emittance growth will be presented. In all cases, these instabilities and beam-breakup modes turn out to be minor and easily kept under control.

Finally, in section 7 a recyclotron design will be shown. The tradeoffs between it and a straight-line machine will be outlined.

2. Electron beam requirements

Simulations of the free-electron lasing interaction have indicated the following minimum quality values for an electron beam entering an undulator [1]:

Wavelength	50 nm	12 nm	4 nm
Energy	250 MeV	500 MeV	750 MeV
Normalized 90% emittance	$\leq$ 40 π·mm·mrad	24 π·mm·mrad	4 π·mm·mrad
Peak current	$\geq$ 100 A	$\geq$ 150 A	$\geq$ 200 A
Energy spread (FWHM)	$\leq$ 0.2%	$\leq$ 0.1%	$\leq$ 0.1%

The required micropulse charge is at least 2 nC within these specifications.

The proposed facility will have a series of FEL oscillators through which the electron beam will pass sequentially (fig. 1). The oscillators, requiring better electron beam quality, are first in the sequence. There will be slight energy extraction from the electron beam in each of the oscillators, hence only slight beam quality degradation. Thus if the electron beam satisfies the requirements for the first oscillator, the beam will still have sufficient quality by the time it reaches any of the latter oscillators to satisfy their less stringent requirements too.

All emittances quoted in this paper refer to the normalized phase-space areas occupied by 90% of the beam's particles. Thus if the beam has a waist with radius r_0 and maximum divergence angle r_0', the emittance will be slightly less than $\gamma \pi r_0 r_0'$.

3. Injector choices

Two choices are possible for the electron injector for an XUV machine. Recent progress in work with conventional injectors using Pierce guns has shown that their brightness is acceptable for an oscillator operating at 50 nm [2]. However, to obtain the beam brightness required for lasing at 12 nm, it appears that a photoelectric injector [3] is needed.

The photoelectric and conventional injectors are very different in design (fig. 2). The photoelectric injector utilizes a cathode in an rf cavity. A laser illuminates the cathode, drawing off typically 200 A for pulse durations around 100 ps. The rf fields in the cavity accelerate the electrons up to 1 MeV. The electrons are immediately injected into more accelerator cavities. A computer simulation of the gun and first rf cavity is shown in fig. 3a.

Much less peak current is available from a conventional thermionic cathode, usually about 5A. Thus to generate 15 nC of charge, a pulse length of 3 ns is required. Because this is too long a time for convenient accelerator rf frequencies, the gun is at a relatively low dc voltage, usually around 100 kV. These low nonrelativistic voltages help facilitate velocity bunching of the beam. Peak current increases of a factor of 100 are common [4]. The long electron pulse (about 50 cm) drifts through lenses and solenoids for focusing. Typically it passes through one or more rf cavities that velocity modulate the beam. Particle overtaking occurs and the beam bunches. Often, the rf cavities have successively shorter wavelengths, for example, a period of about 10 ns (frequency of 100 MHz). As the beam drifts, it becomes shorter and the next cavity can have a period of a few nanoseconds, and so on until the beam is sufficiently bunched to

fit within a few degrees of the rf phase of the accelerator structure. A computer simulation of this type of gun is shown in fig. 3b.

Although the normalized beam normalize emittances leaving the guns based on either a thermionic or photoelectric cathode are similar (about 10 π·mm·mrad), the intrinsic emittance from a photoelectric injector is typically lower because use of the photoelectric injector eliminates the need for a long drift at low voltages. It is well known (see ref. [5]) that the emittance growth from space-charge forces scales as

$$\varepsilon \sim \frac{I}{\gamma^2} G(r,l)\, z \ ,$$

where I is the beam current, γ the usual relativistic mass factor, G (r, l) is a geometric form factor depending on the beam radius and bunch length, and z is the length of the drift region. Comparing the conventional injector to the photoelectric injector, the beam current ratio varies from 1/40 to unity, γ is smaller by a factor of 3, and z is larger by a factor of 20. Taking an average ratio of the beam currents of 1/3, we see that there is typically 60 times more emittance growth in the conventional injector caused by space charge. The other major mechanism for emittance growth in the drift region is the difference in particle focusing caused by the varying beam current along the pulse. This emittance growth scales linearly with the length of the drift region. Again, we see far more emittance growth with the conventional Pierce gun.

4. Design using photoelectric injector

The photoelectric injector has a lower intrinsic emittance; therefore, it was chosen as the primary injector for the new machine. However, this technology is relatively new; thus we are studying a backup injector with a conventional Pierce gun, which will be described in section 5.

The rf cavity (fig. 3a) was designed so that the radial rf electric field was linear.[6] Thus if the electron pulse is sufficiently short enough to eliminate the time variation in the rf fields, the emittance is due only to the nonlinear space-charge fields. Particle-in-cell code simulations indicate that typical initial emittances are <20 π·mm·mrad. Experimentally, even better emittances have been measured. The longitudinal pulse distribution is assumed to be Gaussian, with a uniform transverse cross section.

Because the beam entering the second accelerating cavity is small and expanding outward, these forces contribute to more emittance growth through the rest of the accelerator, particularly in the drift region before the second accelerating cavity. The XUV machine does not require large total charges; a total of 3.5 nC was emitted from the cathode (60 A for 60 ps). Typical emittances at the end of an 11-MeV, 433-MHz linac section following the first cavity for the above parameters are 60 π·mm·mrad. These numbers are larger than is acceptable for lasing at 12 nm, but an emittance filter can be used to regain satisfactory emittance.

There is no longitudinal mixing of the particles as there would be with velocity modulation and bunching. Thus the bunch's front and end particles have consistently experienced less radial electric field than the ones at the bunch's center. The emittance growth is mostly because these particles have gained less outward radial velocity than the others. Also, depending somewhat on the bunch's longitudinal distribution, the ratio of fractional total charge that they constitute to the additional area of phase space they occupy is usually low, say $< 1/3$. Thus, a major drop in emittance with only a small penalty in decreased charge (and virtually no drop in peak current) is possible if we can remove these particles.

An aperture is the best type of emittance filter. Focusing the beam to a crossover by external solenoids, the end particles will form a beam waist at an early axial position, and the waist formed by the particles at the bunch's center will be at a later axial position. Thus if we put an aperture on the other side of the crossover, we can scrape off the front and rear particles but let the more well-behaved central ones through. Filtering with this kind of arrangement and with the beam described above will drop the emittance from 60 to 24 π·mm·mrad while only losing 1/3 of the total charge (keeping 2.3 nC) (fig. 4). Of course this scraping must be done at a high enough energy that the additional space-charge emittance growth is negligible. For emittances down to 20 π·mm·mrad, 12 MeV appears to be sufficient.

Magnetic bunching can be used to increase the peak current from 60 A to levels acceptable for lasing at 12 nm (150 A). A nonisochronous section can be built with dipoles (fig. 5) in which the more energetic particles have a shorter path length. An rf cavity phased for nonacceleration can put a linear energy ramp on the particles (fig. 6); therefore, the particles in front have less energy. Bunching then will occur in the nonisochronous section and, by varying the amount of energy variation front to end of the pulse, different final peak currents can be obtained. With the bend shown in fig. 5, the nonlinear terms in the transport limit the final peak current to just over 400 A (fig. 7). With a more careful design of the nonisochronous section, the nonlinear terms

could be reduced, and the final peak current would be limited by the previous energy spread in the bunch caused by the space charge (yielding 800 A). At 12 MeV, 1 π·mm·mrad emittance growth is seen for 400 A of bunched current. To bunch to higher peak current, say 1 kA, 15 or 16 MeV might be required.

After bunching, the bunch length is quite short; therefore, additional linac tanks at 1.3 GHz can be used to accelerate the beam to 500 MeV (fig. 8) or to the final energy desired. No additional beam degradation is seen. The final phase and energy histograms and phase-space plots are shown in fig. 9. The peak current is 150 A, energy spread is 0.08%, and emittance is 24 π·mm·mrad.

Thus the photoelectric injector appears easily to meet the requirements for lasing at 12 nm with a Gaussian electron-pulse shape. Using a trapezoidal pulse shape instead, there is less difference in the radial electric field at the different locations within the pulse and this, in turn, causes less emittance growth. With a 60-A peak and 80-ps FWHM pulse, there is less emittance growth through the first 12-MeV section, and (in particular) the central section of the bunch does not degrade. By scraping different amounts by varying the aperture diameter, we can generate this listing of emittances versus transmitted current:

Percent Electrons Transmitted	Charge Transmitted	Emittance (π•mm•rad)
100	5.0	52.3
85	4.3	31.2
65	3.3	15.1
50	2.5	9.3
40	2.0	5.5
30	1.5	4.5
18	1.0	2.5

Although the useful charge is lower than desired (<2nC), we see emittances <4 π·mm·mrad. Scaling the magnetic phase compressor to limit the emittance growth from 3 to 4 π from the above data shows that the beam energy only has to be

14 MeV. If the bunching takes place at higher energy, there will be less emittance growth.

5. Conventional injector backup

Although use of the photoelectric injector to meet the lasing requirements at 12 nm seems to be straightforward, the technology involved is new, and we have designed a backup injector using a conventional Pierce gun. With the conventional injector, the 50-nm requirements appear to be achievable (they are less strenuous than some published results [2]), and the requirements for lasing at 12 nm may be met with additional beam filtering.

We start with a planar Pierce gun. The intrinsic emittance from a 3-ns, 5-A pulse is good, about 20 π·mm·mrad. We can compare this to the smaller beam from a spherical Pierce geometry with an emittance of about 10 π·mm·mrad (fig. 10). Although the initial emittance is less, the smaller beam expands more rapidly in the 80-kV drift section and the final emittance is higher.

Using the same injector design as in the Los Alamos FEL energy recovery experiment [7], we can deliver a beam with 200 A, emittance <40 π·mm·mrad, and an energy spread of $<0.1\%$ at 500 MeV, satisfying nicely the 50-nm requirements (fig. 11). There is roughly 8 nC in the delivered pulse, which is more than needed. By more emittance filtering, we can halve the emittance, and with further magnetic bunching we can still maintain 200-A peak current with 3 nC.

6. Emittance growth in the beamline and undulators

We have studied these emittance growth mech .nisms:

(1) Emittance growth caused by wake fields in beamline bends
(2) Emittance growth caused by cumulative beam breakup in the 500-MeV linac
(3) Emittance growth that is due to nonachromatic bends between the undulators
(4) Emittance growth caused by the transverse resistive wall instability in the undulators

6.1. Emittance growth caused by wake fields in beamline bend

This emittance growth mechanism is important usually only for bends with large discontinuities. One possible such discontinuity would be a hole to let the laser light out as the beamline bends away from the optical axis. This mechanism is well understood [4]. It will be negligible for the beam used in an XUV FEL. We have experimentally studied this with a 20-MeV, 10-ps electron bunch with 600-A peak current. By using a large rectangular pipe so the bunch's corresponding wall currents were kept far away from the perturbing hole, we were able to show the emittance growth was less than 100 π·mm·mrad. Because the emittance growth scales as l/γ, in the case of the XUV beam we could expect 1/75 as much an effect, or well less than 1 π·mm·mrad emittance growth.

6.2. Emittance growth caused by cumulative beam breakup in the 500-MeV linac

The designed average current of the XUV FEL is 300 mA during a 300-μs macropulse. The calculated emittance growth that is due to the cumulative beam breakup is negligible for 1% beam jitter (explained below) at 500 MeV with the focusing elements providing 45° phase advance between accelerator tanks, with 1-MHz staggered tuning, and with the cavities phased sufficiently nonresonant to reduce the effective shunt impedance of the breakup mode to <75% of the maximum (see fig. 12). The 1% jitter refers to a 1% uncertainty in the transverse position of the beam from one pulse to the next. The maximum shunt impedance was calculated from the code URMEL.

6.3. Emittance growth that is due to nonachromatic bends between the undulators

To preserve the good emittance between undulators, a beam transport system as shown in fig. 13 has been designed to be installed between wigglers. The design is both achromatic and nearly isochronous (fig. 14). Details of this design can be found in ref. [8].

6.4. Emittance growth caused by the transverse resistive wall instability in the undulators

The transverse resistive wall instability leads to a variation of beam position along the beam pulse [9]. This in turn can be interpreted as an effective emittance growth. Fig. 15 shows the increase in beam size for various beampipe sizes in the undulator for both 30- and 300-mA macropulse average currents. We assume 300-μs pulse lengths with 1% beam jitter and a 500-MeV linac. What fig. 15 really indicates is (1) the maximum tolerance on the transverse beam displacement is one-tenth the beam size in the undulator (beam radius is 200-500 μm), (2) if the tolerance cannot be met, the undulator beampipe size should be increased. The data shown in fig. 15 were calculated assuming a beampipe wall of infinite thickness. Recent results (ref. [10]) show that the instability is greatly reduced for beampipe of finite wall thickness because of the magnet field penetration of the beampipe wall.

7. Recyclotron versus straight linac

The two main advantages of using a recyclotron design (fig. 16) are (1) less accelerator structure is needed and a smaller building can be used to house it and (2) less rf power (thus less electrical cost) would be required to run it. However, there are in addition these disadvantages: (1) more bends (all 180°) including several at lower energy that would be more sensitive to emittance growth, (2) average current is limited by the regenerative beam breakup (using formulas in ref. [11] the worst-case thresholds are 5 mA for a six-pass, 500-MeV machine (8 mA for 4 passes) and 25 mA for a three-pass, 250-MeV (50 mA for 2 passes) machine—real threshold currents are typically 10-100 times larger), and (3) a recycling machine usually requires a longer time to configure and commission.

8. Summary

The conclusion from the accelerator design work is that, using the photoelectric injector, an accelerator can be built that meets the requirements for lasing down to 12 nm without representing a significant extension of technology, thus with little risk. A conventional Pierce gun can be used to obtain lasing down to wavelengths of 50 nm.

In addition, the photoelectric injector may be useful down to wavelengths of 4 nm for a self-amplified spontaneous emission amplifier and the Pierce gun to wavelengths of 12 nm.

Also, beam instabilities and breakup seem to be controllable for the peak and average currents needed for the XUV FEL.

Finally, the savings in cost with building a recycling machine must be weighed against the extra risk of beam degradation.

There are still several areas for further work. We want to examine different operating regimes of the photoelectric injector to see if we can realistically obtain emittances of 4 π·mm·mrad at the end of a 750-MeV linac.

More wake-field calculations are required to make sure the minimum effect from pipe discontinuities is seen from the point of energy spread and emittance. Also, an integrated accelerator and beamline design has yet to be finalized.

Acknowledgment

We wish to acknowledge several helpful discussions with J. Fraser, M. Jones, B. Newnam, and R. Sheffield.

References

[1] J. C. Goldstein and B. D. McVey, "Recent Theoretical Results for an RF-Linac-Driven XUV Free Electron Laser," Eighth International Conference on Free-Electron Lasers, Glasgow, Scotland, September 1-5, 1986, to be published.

[2] J. C. Adamski, W. J. Gallagher, R. C. Kennedy, D. R. Shoffstall, E. L. Tyson, and A. D. Yeremian, "Accelerator Technology for a High Power Short Wavelength FEL," SPIE, 453, 59, (1984).

[3] J. S. Fraser, R. L. Sheffield, E. R. Gray, P. M. Giles, R. W. Springer, and V. A. Loebs, "Photocathodes in Accelerator Applications," 1987 Particle Accelerator Conference, Washington, DC, March 16-19, 1987, to be published.

[4] B. E. Carlsten, D. W. Feldman, A. H. Lumpkin, J. E. Sollid, W. E. Stein, and R. W. Warren, "Emittance Studies at the Los Alamos National Laboratory Free-Electron Laser," these proceedings.

[5] M. E. Jones and B. E. Carlsten, "Space-Charge Induced Emittance Growth in the Transport of High-Brightness Electron Beams," 1987 Particle Accelerator Conference, Washington, DC, March 16-19, 1987 to be published.

[6] M. E. Jones and W. K. Peter, "Particle-in-Cell Simulations of the Lasertron," IEEE Trans. Nucl. Sci. 32 (5), 1794 (1985).

[7] D. W. Feldman, R. W. Warren, J. M. Watson, W. E. Stein, J. S. Fraser, G. Spalek, A. H. Lumpkin, B. E. Carlsten, H. Takeda, T. S. Wang, and C. A. Brau, "The Los Alamos Free-Electron Laser Energy Recovery Experiment," 1987 Particle Accelerator Conference, Washington, DC, March 16-19, 1987, to be published.

[8] Design of a Beam Transport System between the Wigglers in the XUV FEL, K. C. D. Chan, Tech. Note of the Accelerator Technology Division, Los Alamos National Laboratory, Los Alamos NM 87545, ATN-86-29, October, 1986.

[9] G. J. Caporaso, W. A. Barletta, and V. K. Neil, "Transverse Resistive Wall Instability of a Relativistic Electron Beam," Particle Accelerators, 11, 71, 1980.

[10] Transverse Resistive Wall Instability of a Bunched Electron Beam in a Wiggler, G. Rangarajan and K. C. D. Chan, Tech. Note of the Accelerator Technology Division, Los Alamos National Laboratory, Los Alamos, NM 87545, ATN-87-25, August, 1987.

[11] J. Bisognano and G. Kraft, "Multipass Beam Breakup in the CEBAF Superconducting Linac," 1986 Linac Conf. Proc., Stanford Linear Accelerator Center report SLAC-303 (1986).

Figure Captions

Fig. 1. Configuration of the proposed Los Alamos XUV/UV FEL (1 to 400 nm). One rf linear accelerator drives multiple, FEL oscillators in series.

Fig. 2. The 50-nm requirements can be met using either a photoelectric injector or a conventional injector.

Fig. 3. Qualitative comparison of the gun regions of the photoelectric and conventional injectors.

Fig. 4. With an aperture, one-third of the electrons are lost and the emittance is decreased from 60 π·mm·mrad to 24 π·mm·mrad.

Fig. 5. Magnetic phase compressor. More energetic particles (1) have shorter path length than less energetic ones (2).

Fig. 6. Magnetic phase compression can be used to obtain currents > 400 A. Nonaccelerating cavity puts an energy ramp on the particles (particles in front of the bunch have less energy than the ones at the rear).

Fig. 7. Magnetic phase compression can be used to obtain currents > 400 A. Particles are passed through a nonisochronous region and the more energetic particles overtake the less energetic ones.

Fig. 8. Example of photoelectric injector with 500-MeV machine that meets the XUV FEL requirements down to 10 nm.

Fig. 9. PARMELA calculations indicate that a 500-MeV linac coupled with the photoelectric injector can obtain currents > 450 A with emittances < 24 π·mm·mrad and energy spreads < 0.1%.

Fig. 10a. Two types of pierce gun geometries that have good intrinsic emittances for 3-ns bunch lengths.

Fig. 10b. Gun trajectory simulations for the two types of geometries.

Fig. 11a. Example of conventional injector in XUV machine using our FEL injector.

Fig. 11b. Conventional injector can meet requirements for XUV FEL down to 50 nm with 250-MeV linac.

Fig. 12. Emittance growth caused by the cumulative beam breakup from random beam jitter is small for reasonable values of the linac sections' shunt inpedance. The maximum shunt impedance is calculated from URMEL. With careful design, an overall impedance of 50% of that value is possible.

Fig. 13. Beam transport design between series XUV FEL undulators preserves emittance.

Fig. 14. PARMELA calculations indicate that the beamline design between undulators preserves transverse emittance and is nearly isochronous.

Fig. 15. Growth in beam size and emittance is due to transverse resistive wall instability, which is very dependent on beam pipe radius through undulator.

Fig. 16. Design for a 250-MeV machine using a recirculating 80-MeV linac.

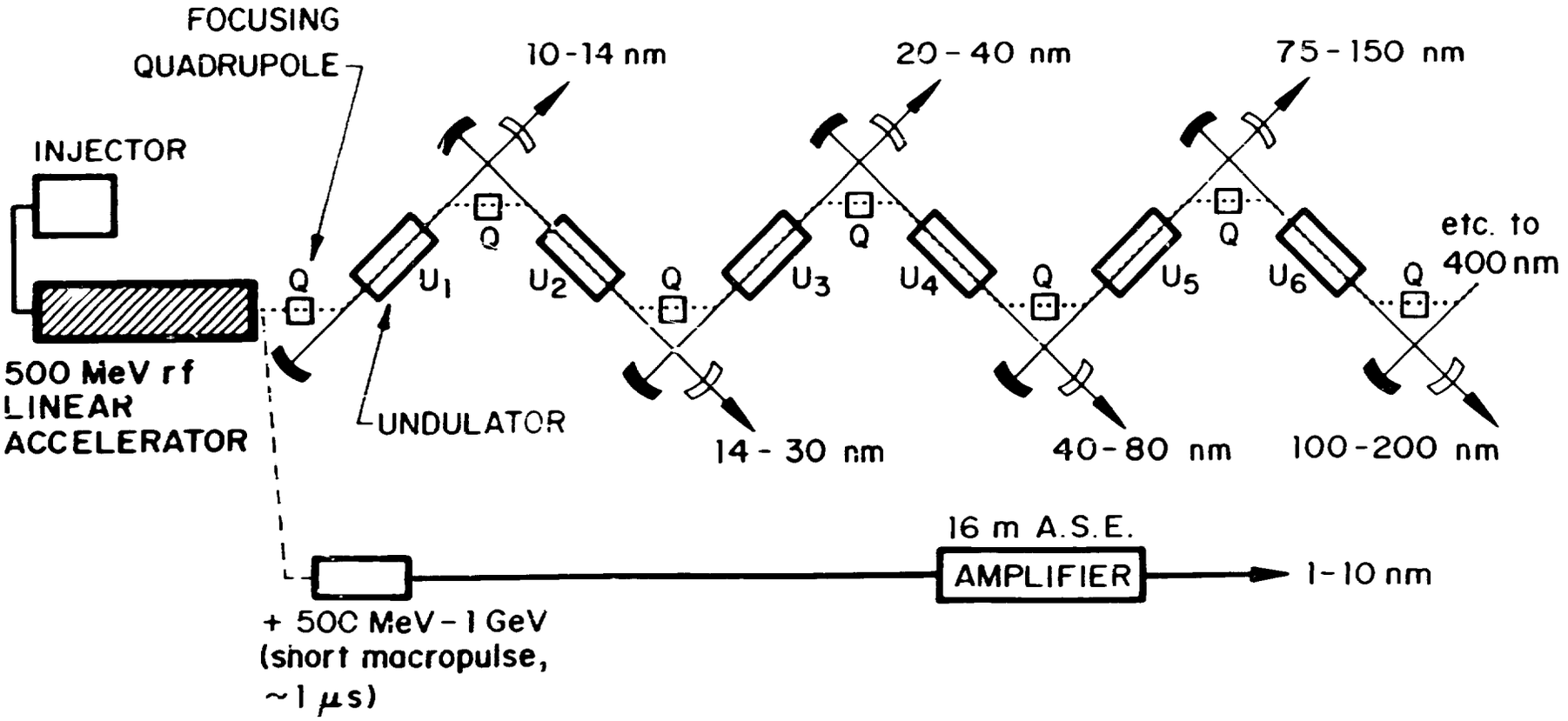
FOCUSING
QUADRUPOLE
INJECTOR
500 MeV rf
LINEAR
ACCELERATOR
Q
U1
U2
U3
U4
U5
U6
UNDULATOR
10-14 nm
14-30 nm
20-40 nm
40-80 nm
75-150 nm
100-200 nm
etc. to
400 nm
16 m A.S.E.
AMPLIFIER
1-10 nm
+ 500 MeV - 1 GeV
(short macropulse,
~1 μs)

CHM-VG-4638 D

Photoelectric injector

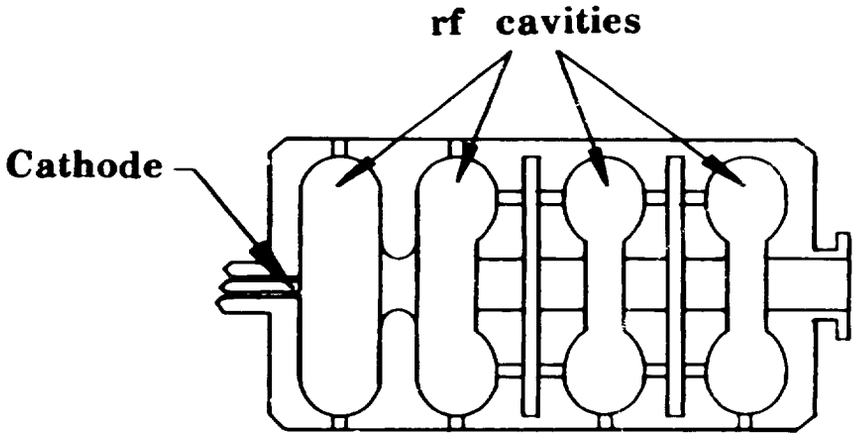

Conventional injector

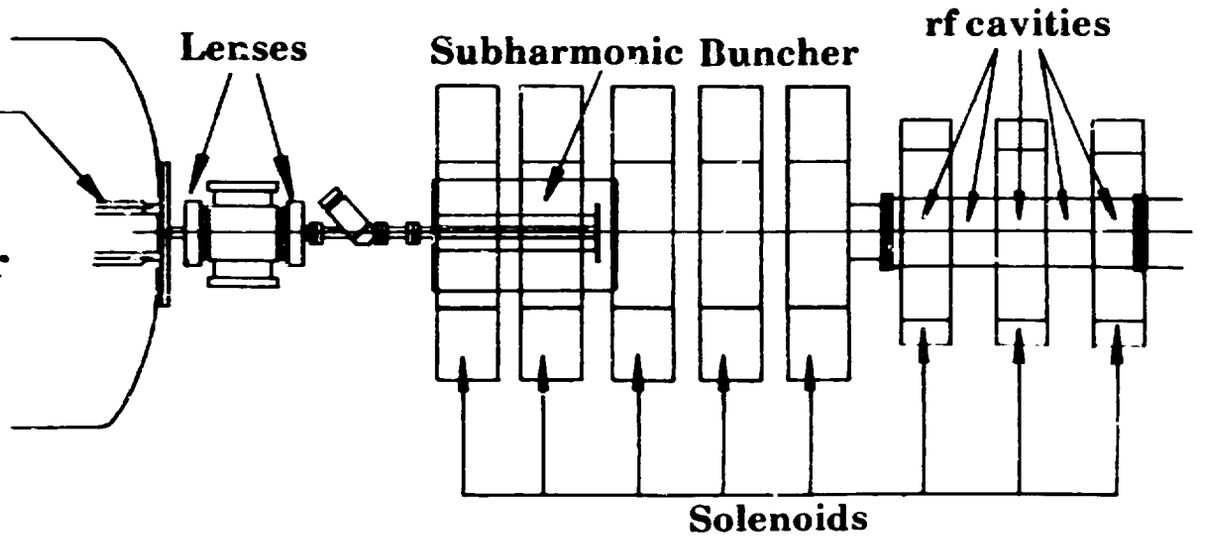

PHOTOELECTRIC

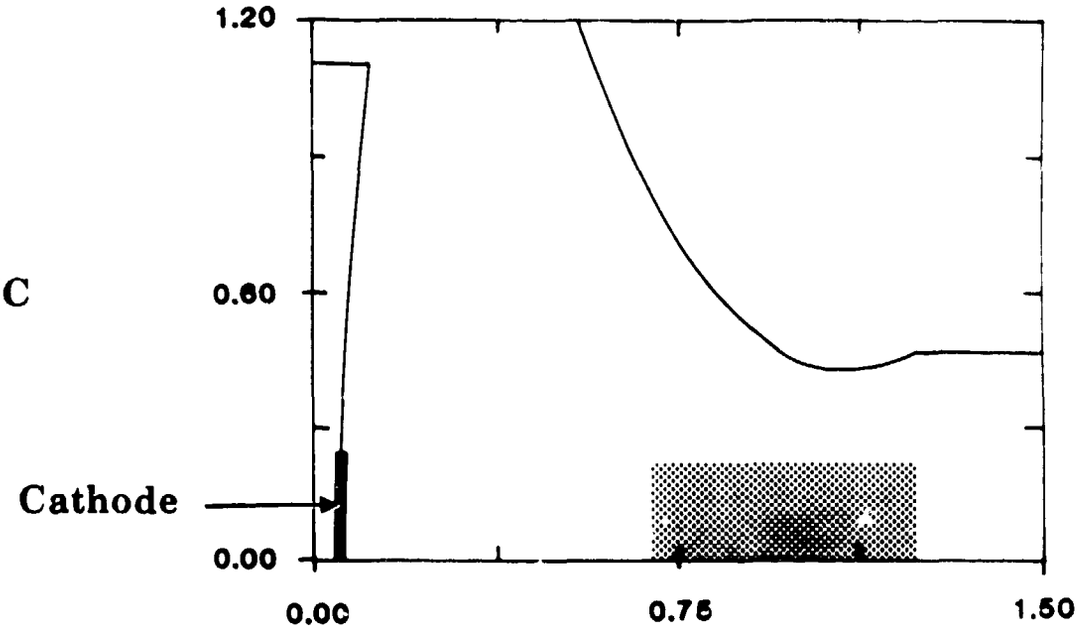

CONVENTIONAL

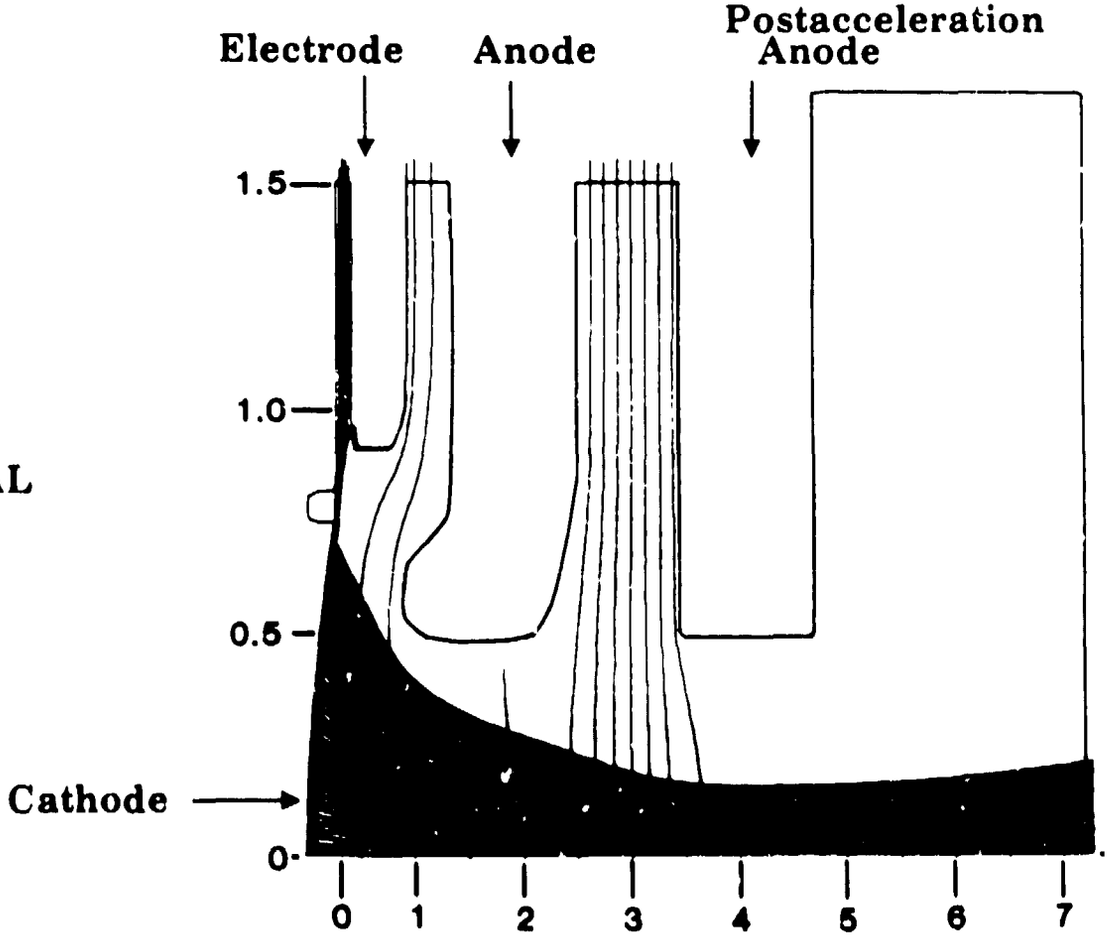

PHASE-SPACE PLOTS

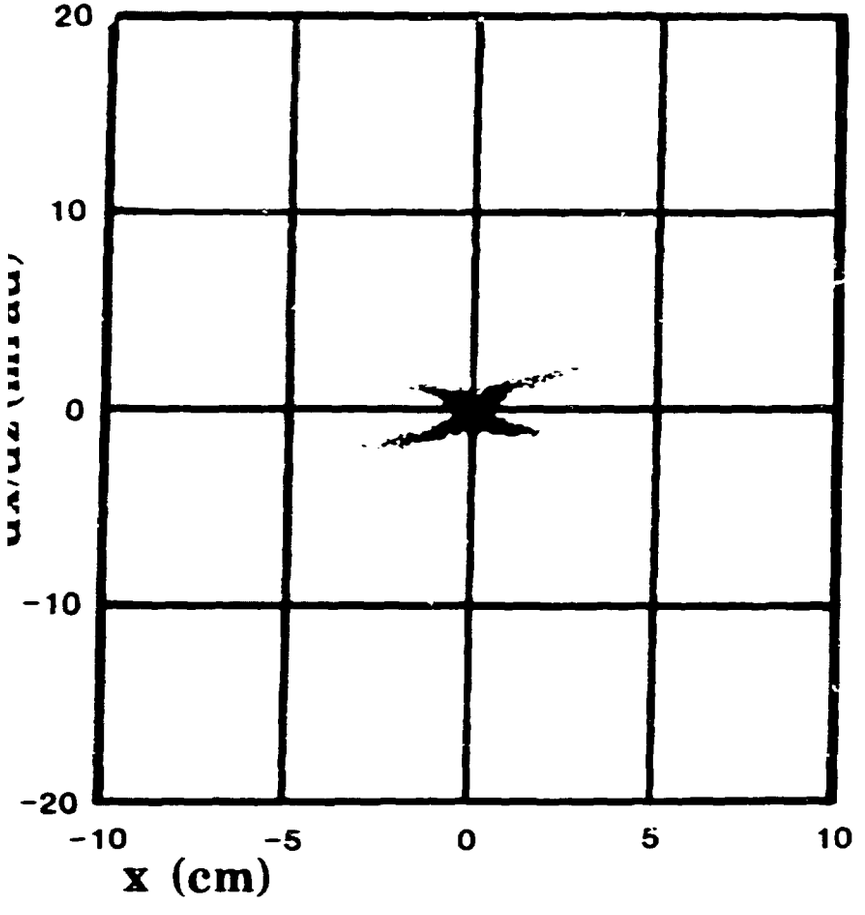

Before aperture

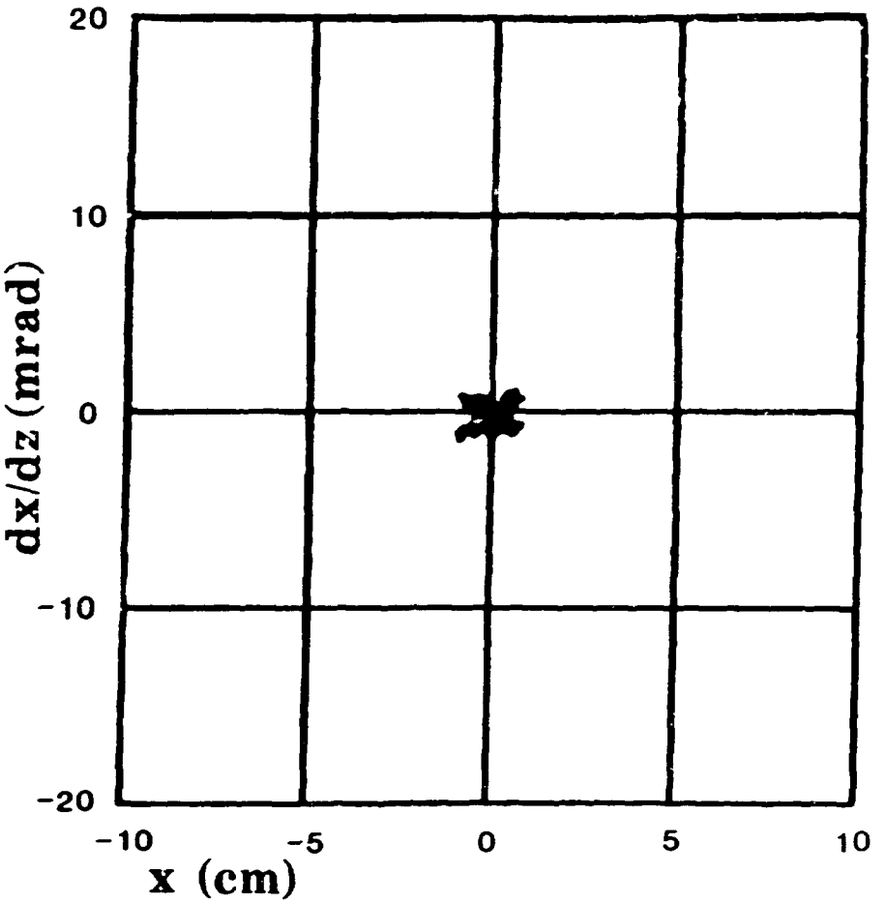

After aperture

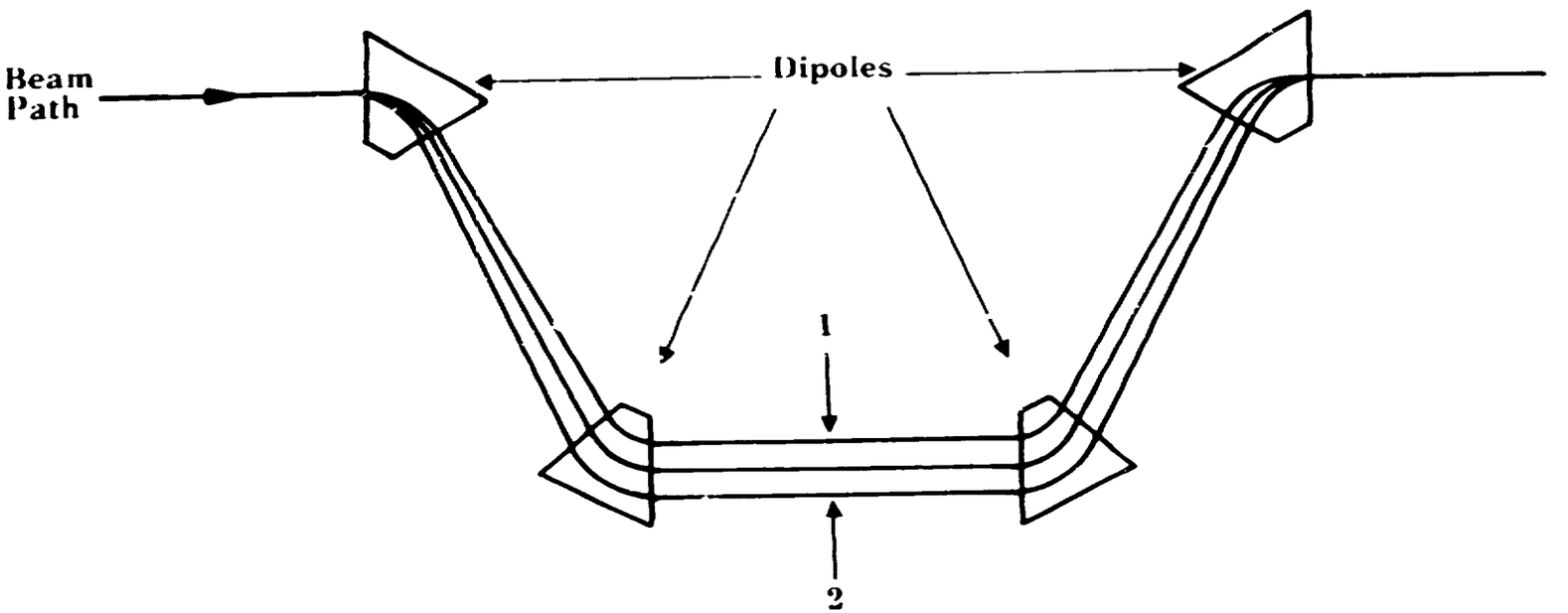
Beam
Path
Dipoles
1
2

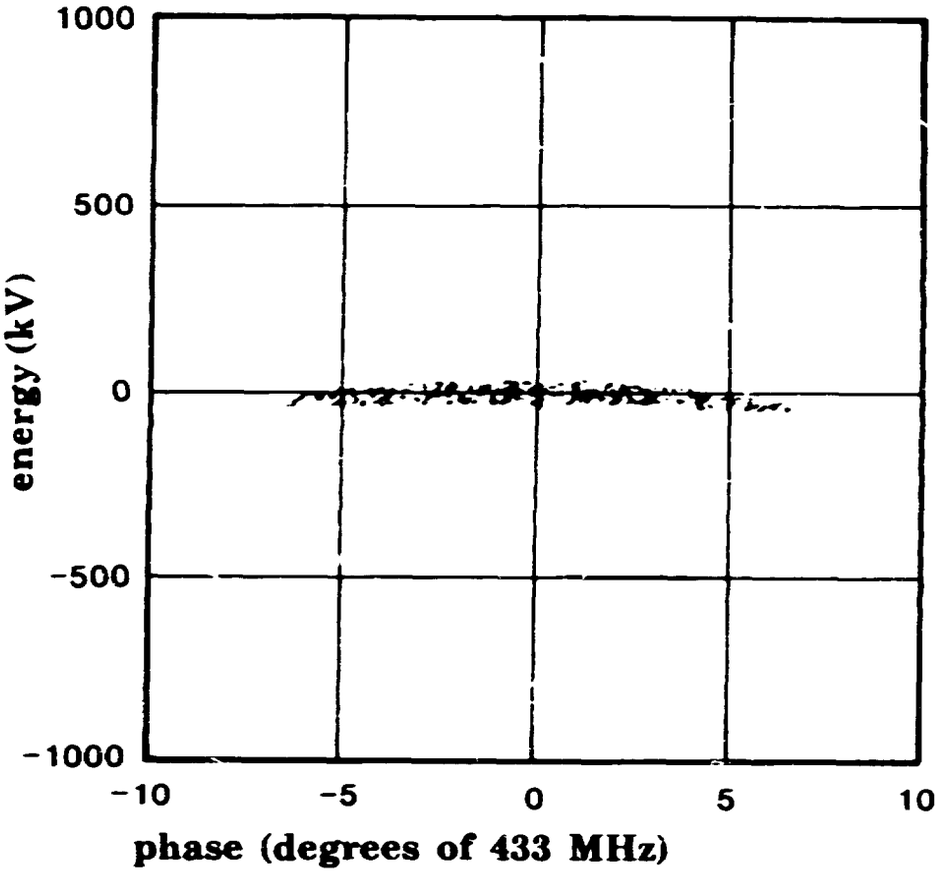

Before ramp cavity

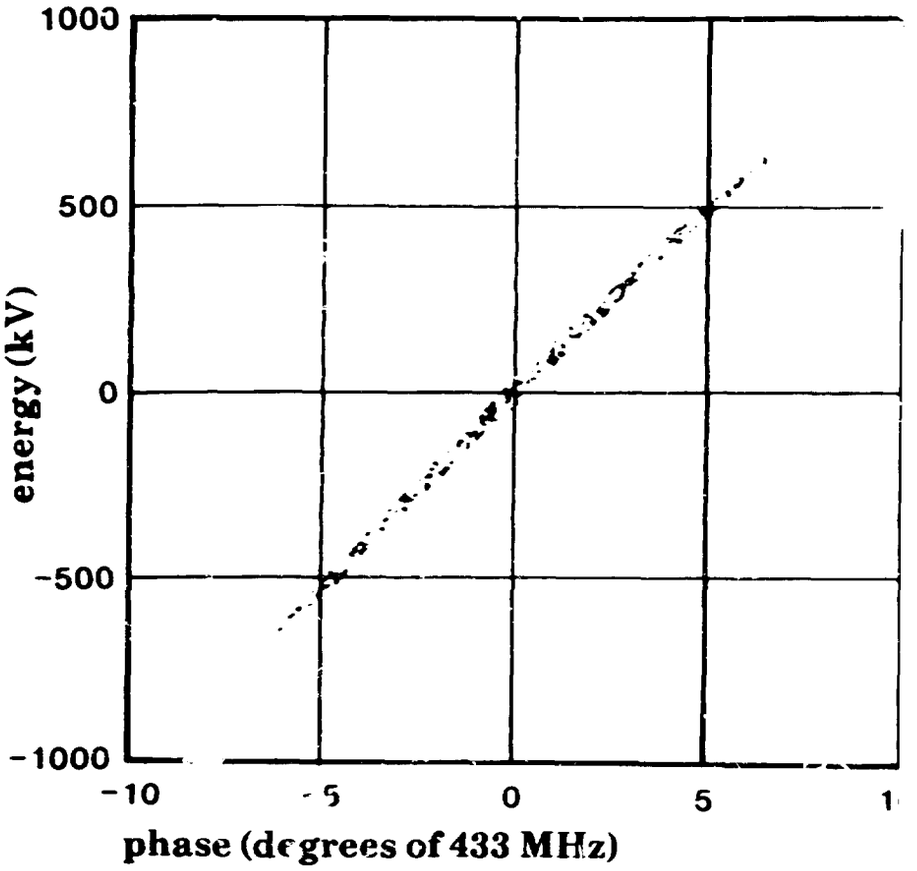

After ramp cavity

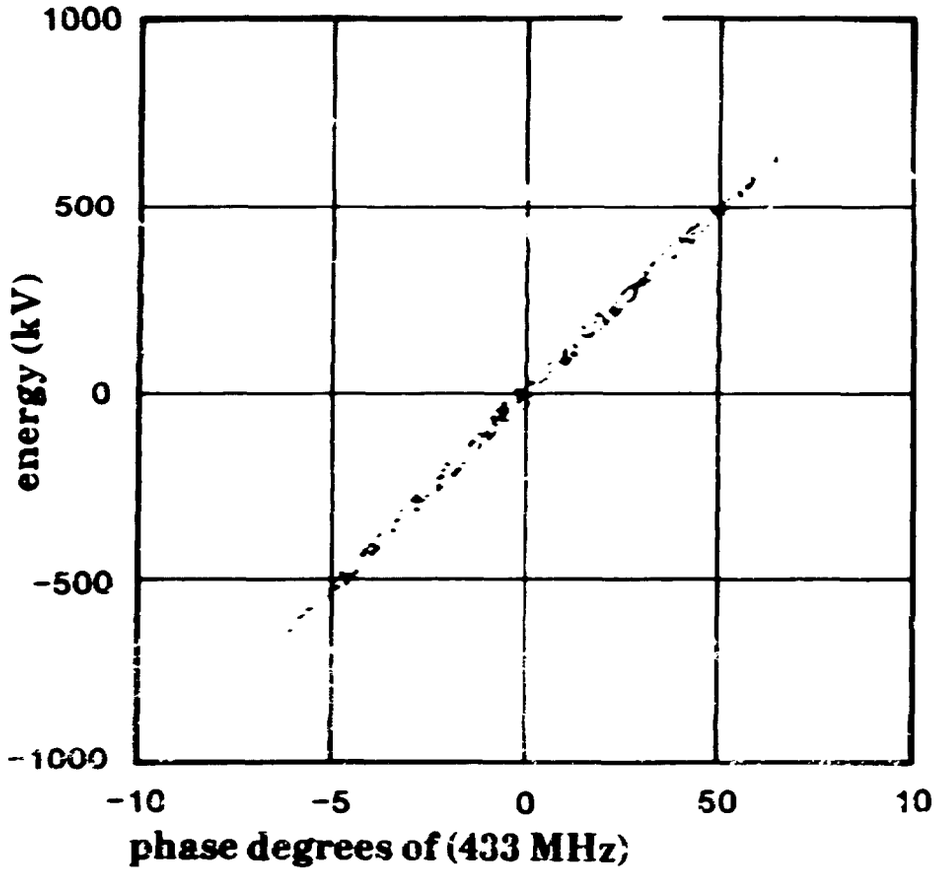

Before nonisochronous region

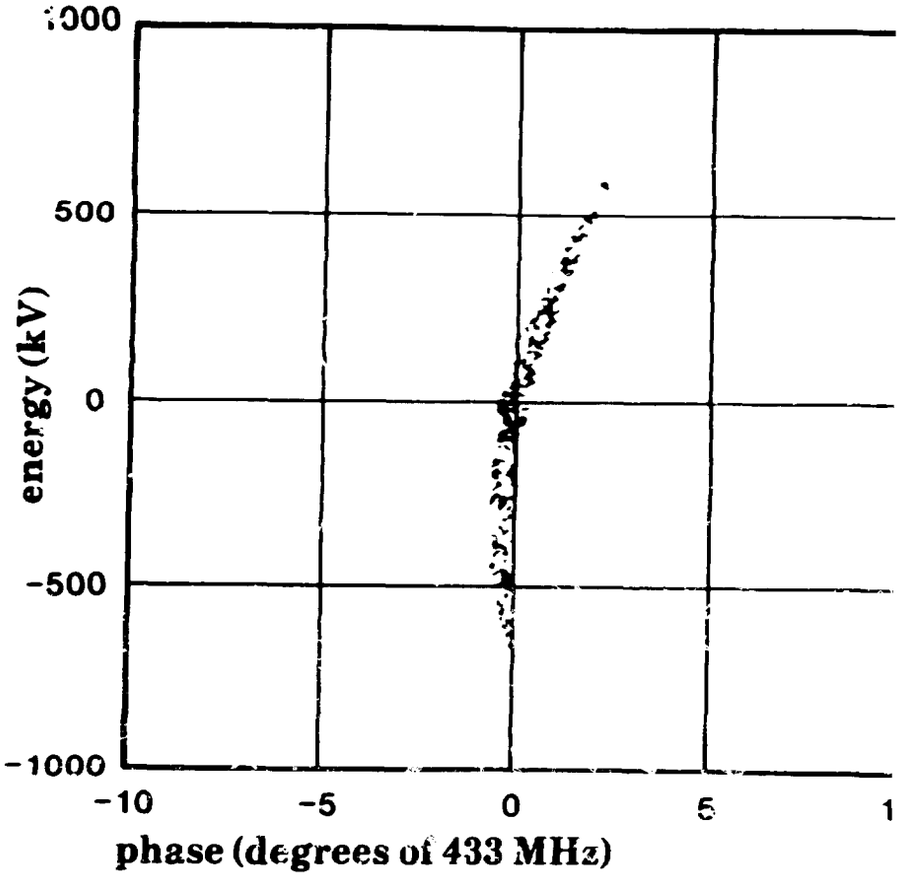

After nonisochronous region

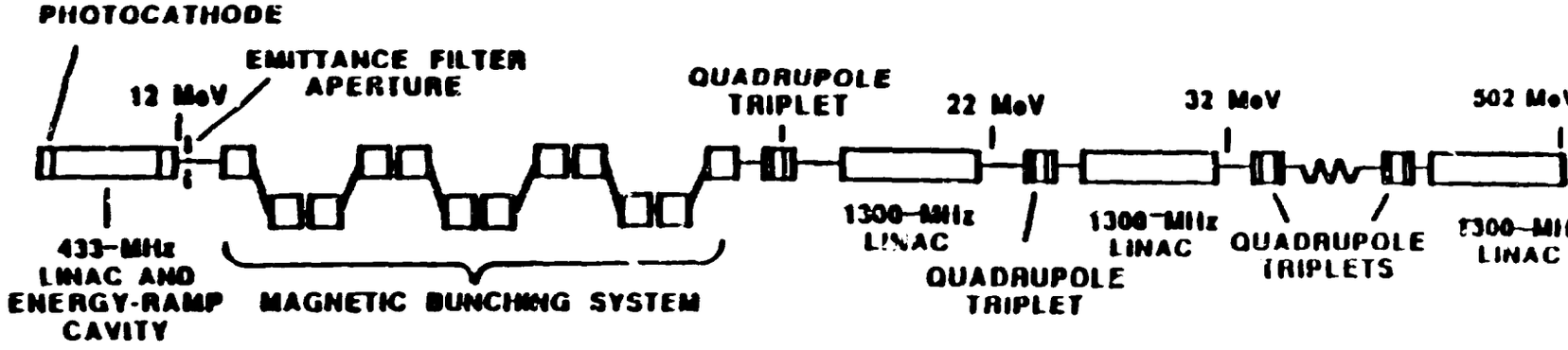
PHOTOCATHODE
EMITTANCE FILTER APERTURE
12 MeV
QUADRUPOLE TRIPLET
22 MeV
32 MeV
502 MeV
433-MHz LINAC AND ENERGY-RAMP CAVITY
MAGNETIC BUNCHING SYSTEM
1300-MHz LINAC
QUADRUPOLE TRIPLET
1300-MHz LINAC
QUADRUPOLE TRIPLETS
1300-MHz LINAC

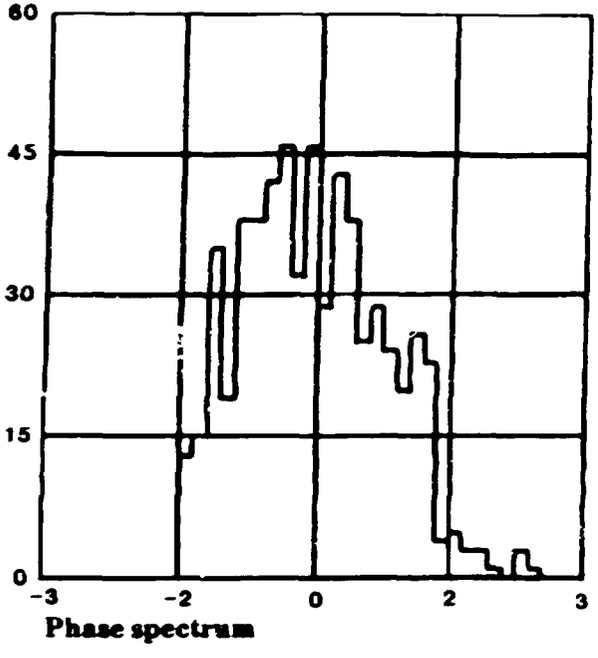

Phase histogram

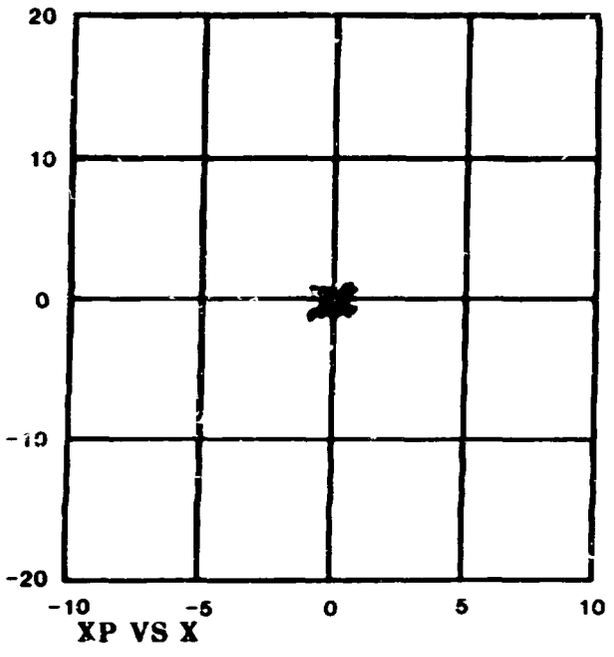

Transverse phase space

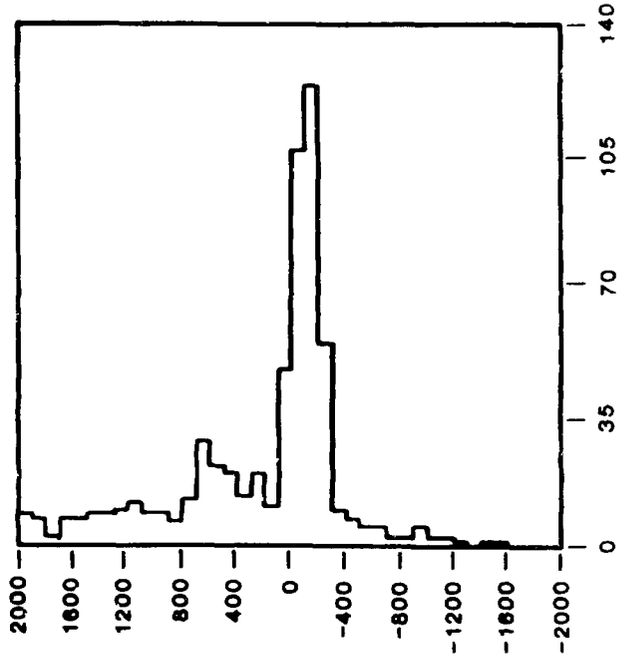

Energy histogram

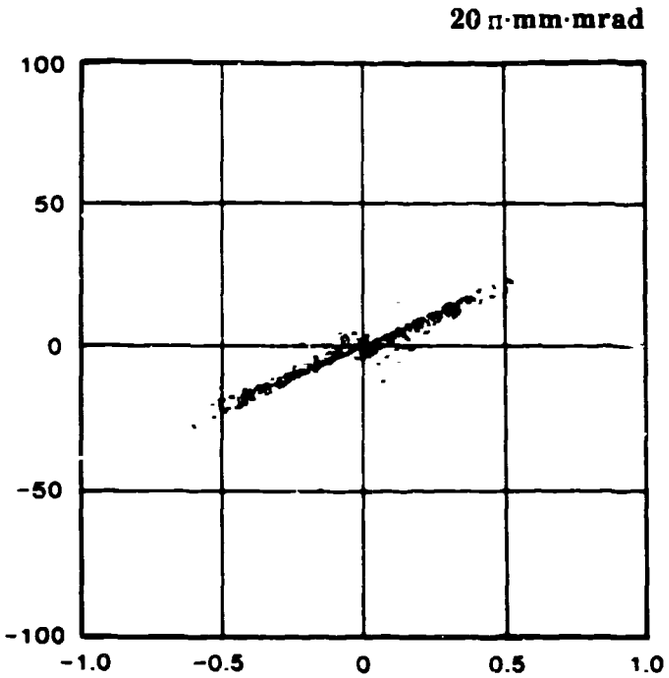

Planar cathode geometry

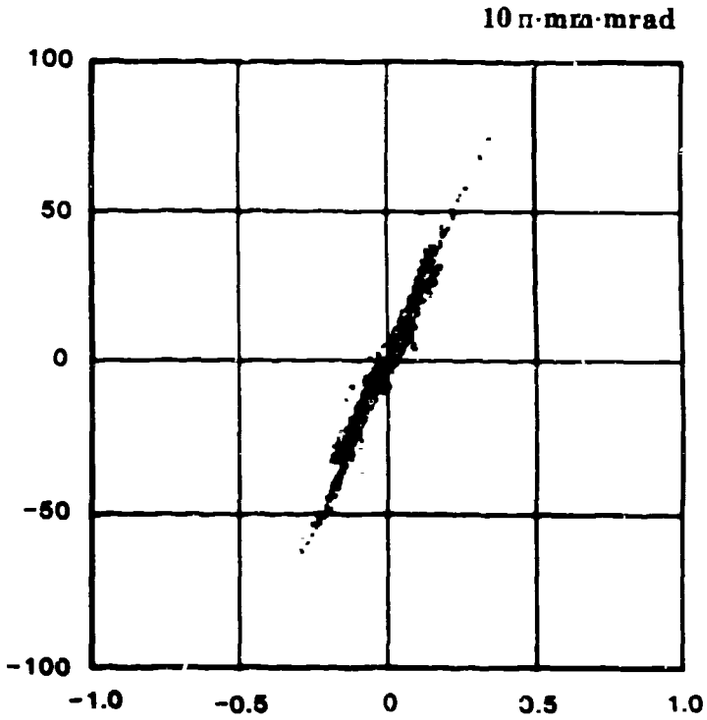

Spherical cathode geometry

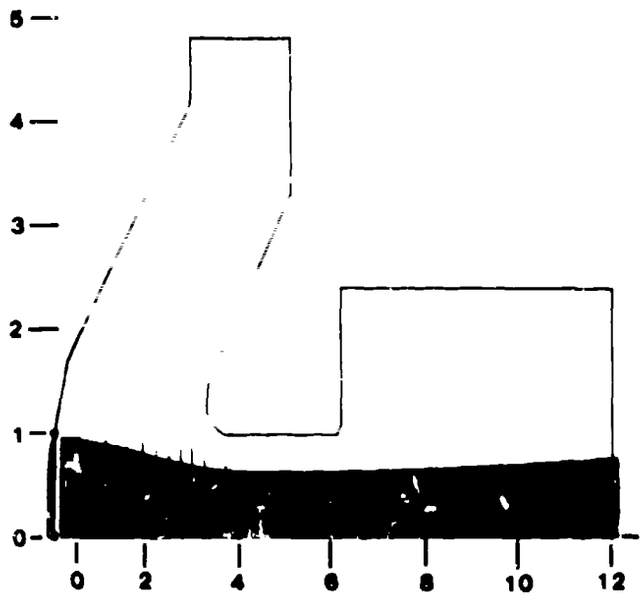

Planar cathode geometry

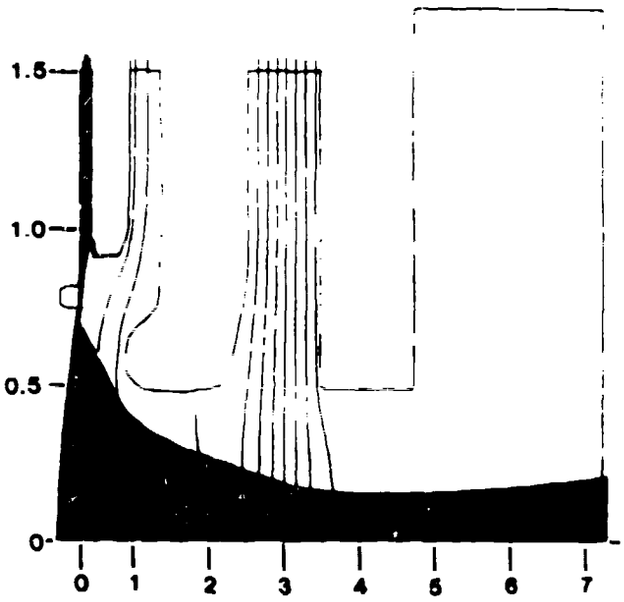

Spherical cathode geometry

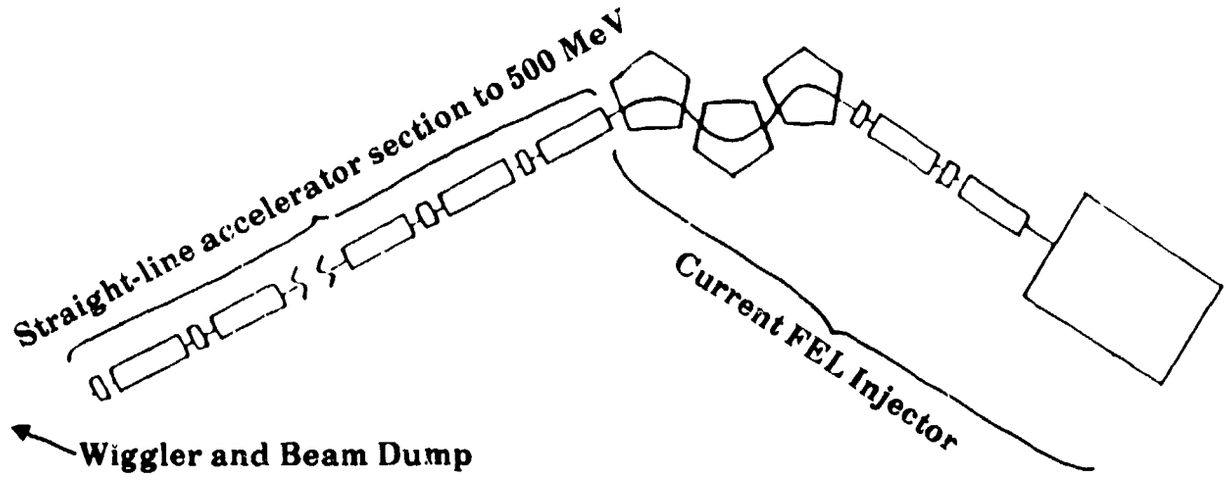

Legend

10-MeV accelerator ▭ ▯ Quadrupole triplet

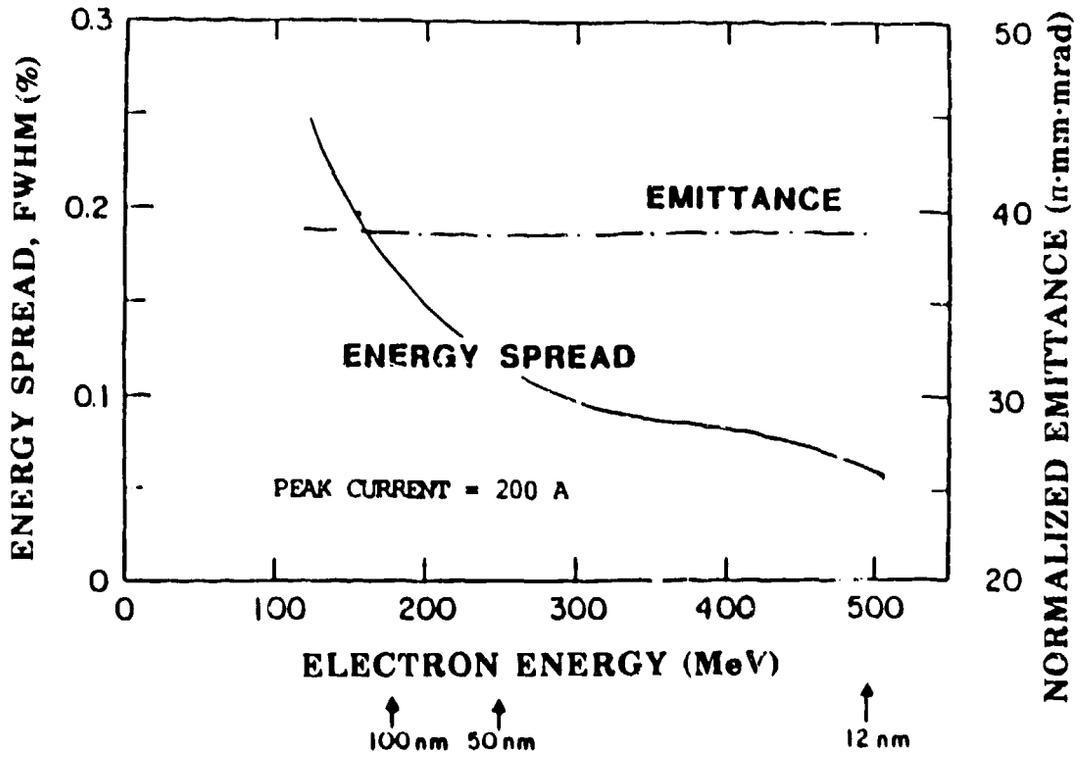

Simulations include longitudinal wako fields induced in rf cavities

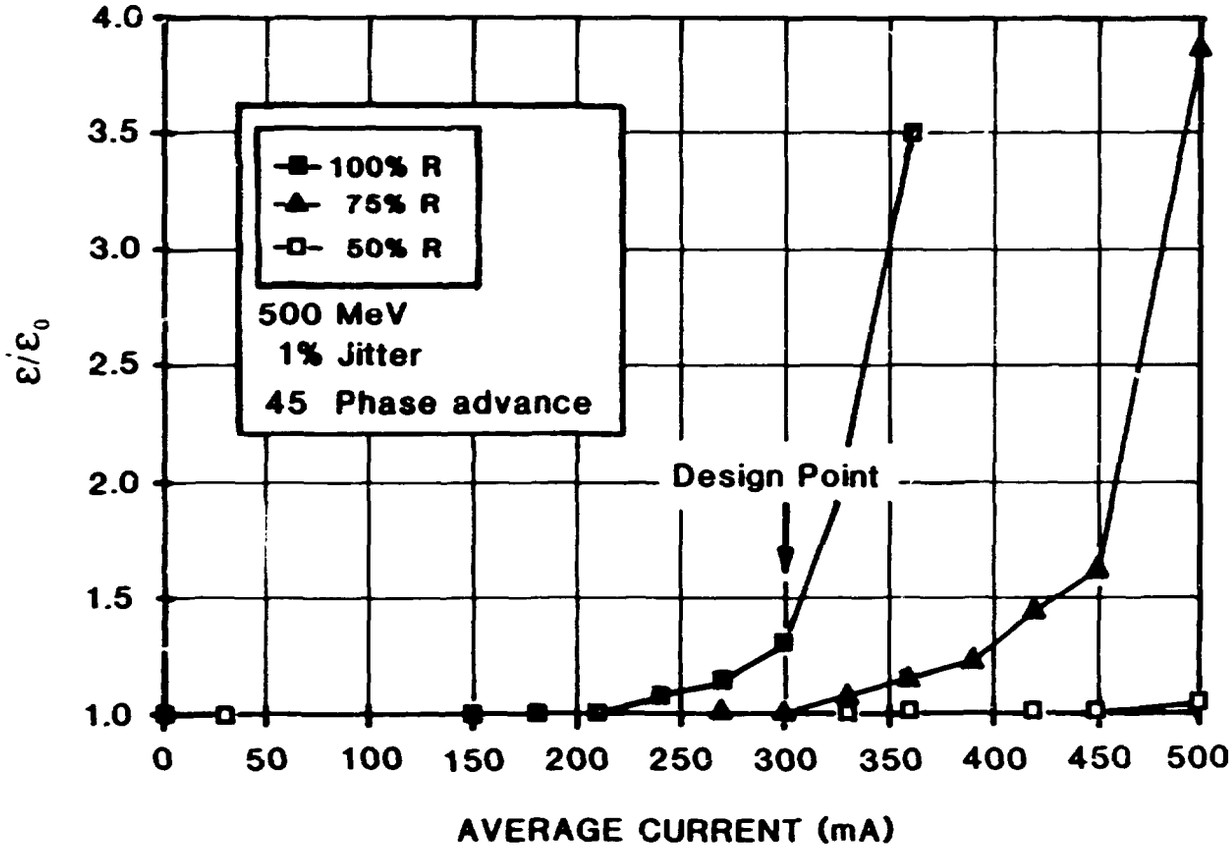
4.0
3.5
3.0
2.5
2.0
1.5
1.0
$\varepsilon/\varepsilon_0$
100% R
75% R
50% R
500 MeV
1% Jitter
45 Phase advance
Design Point
0
50
100
150
200
250
300
350
400
450
500
AVERAGE CURRENT (mA)

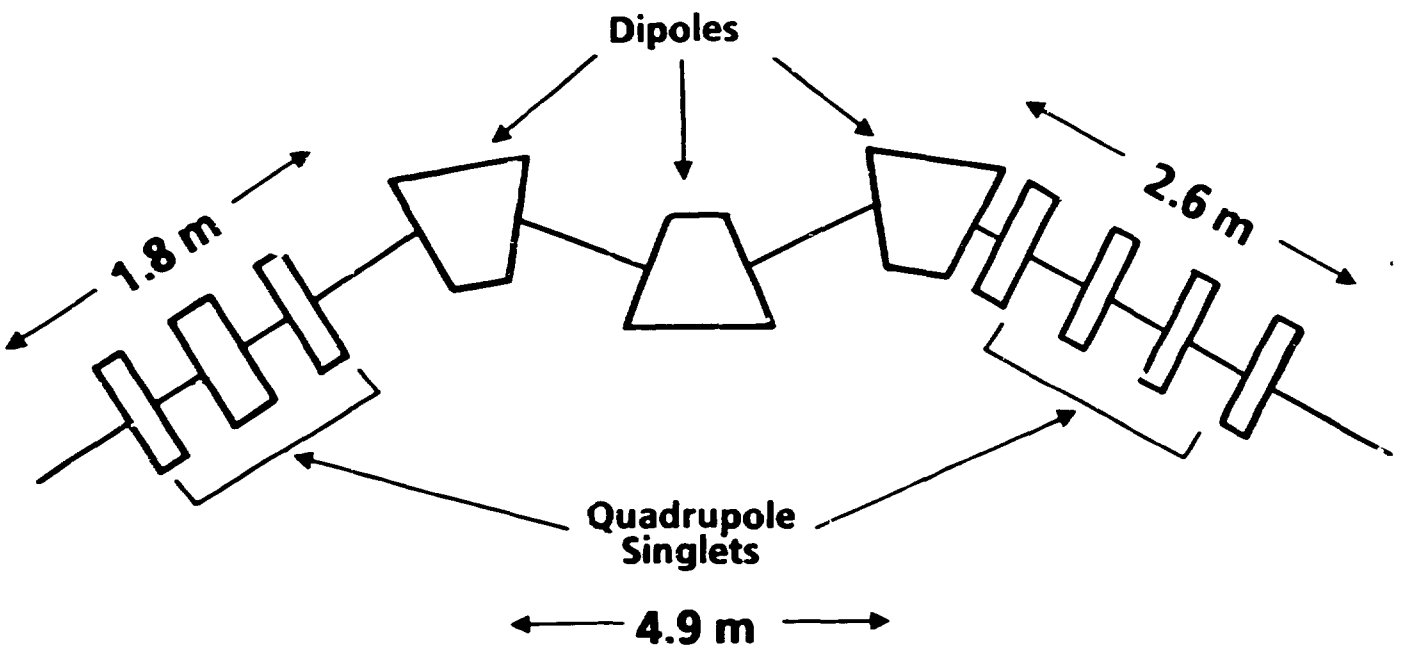
Dipoles
1.8 m
2.6 m
Quadrupole
Singlets
4.9 m

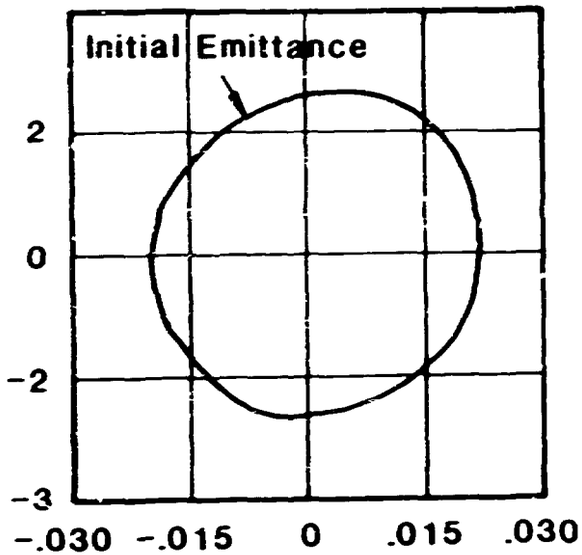

Final Transverse Phase Space

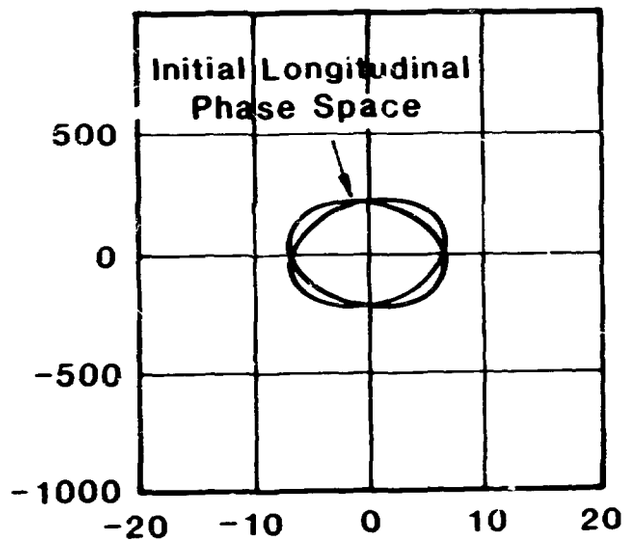

Final Longitudinal Phase Space

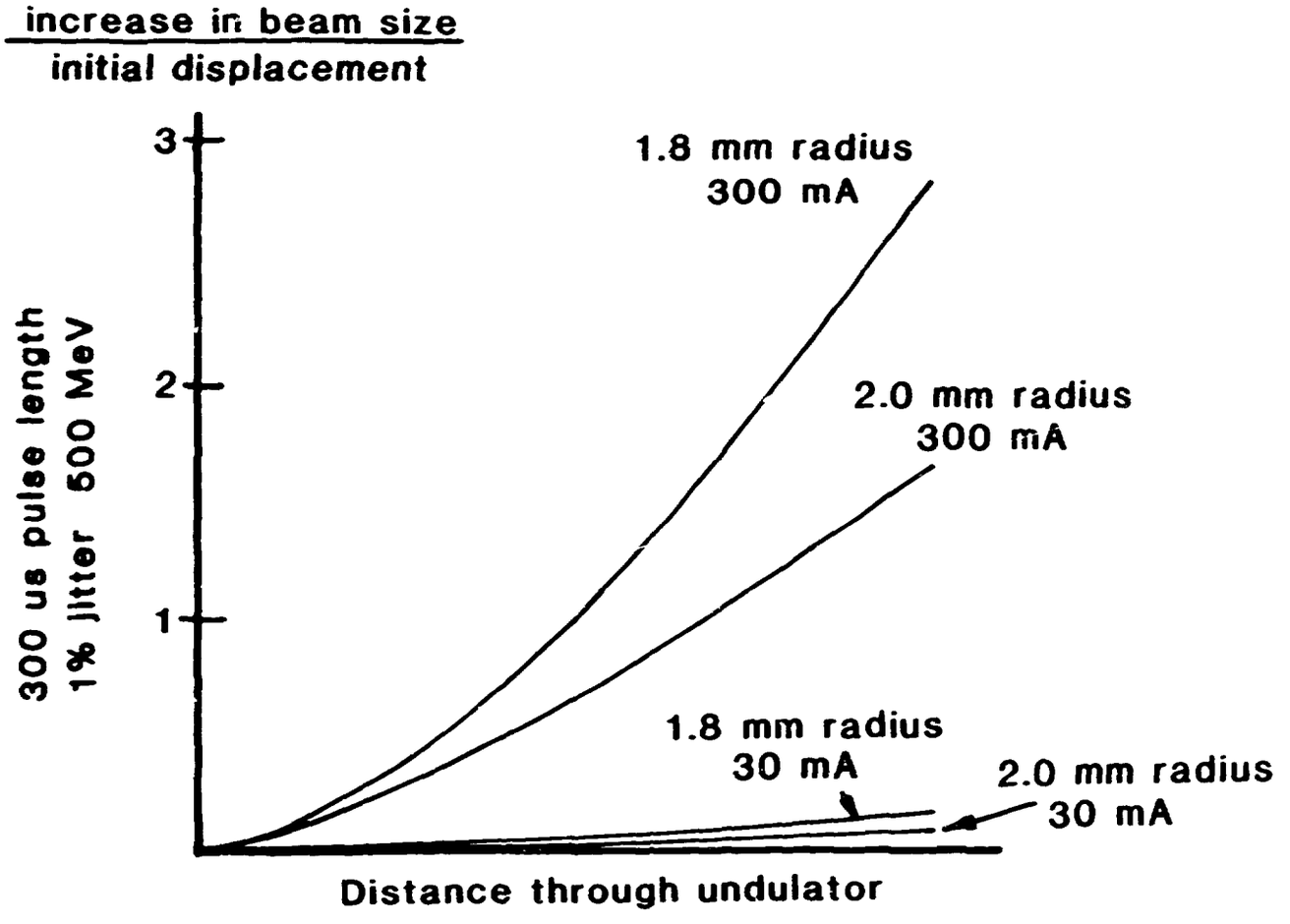
increase in beam size
initial displacement
3
2
1
300 us pulse length
1% jitter 500 MeV
1.8 mm radius
300 mA
2.0 mm radius
300 mA
1.8 mm radius
30 mA
2.0 mm radius
30 mA
Distance through undulator

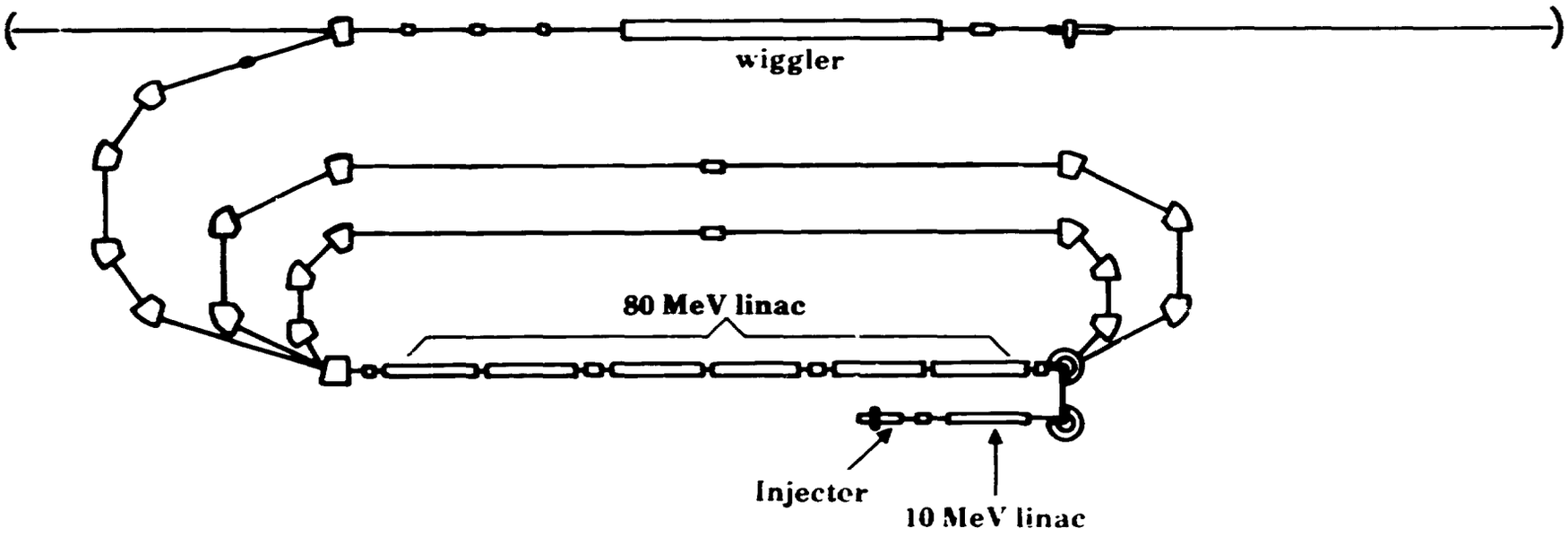
wiggler
80 MeV linac
Injecter
10 MeV linac